Naval Research Laboratory

Washington, DC 20375-5000

NRL Memorandum Report 6895

Stress Field Variations During Dynamic Loading

VIRGINIA G. DEGIORGI

Mechanics of Materials Branch
Materials Science and Technology Division

October 18, 1991

REPORT DOCUMENTATION PAGE

Form Approved
OMB No 0704-0188

1. AGENCY USE ONLY *(Leave blank)*	2. REPORT DATE	3. REPORT TYPE AND DATES COVERED
	1991 October 18	

4. TITLE AND SUBTITLE

Stress Field Variations During Dynamic Loading

5. FUNDING NUMBERS

PE: 61153N
PR: RR022-01-48

6. AUTHOR(S)

Virginia G. DeGiorgi

7. PERFORMING ORGANIZATION NAME(S) AND ADDRESS(ES)

Naval Research Laboratory
Washington, DC 20375-5000

8. PERFORMING ORGANIZATION REPORT NUMBER

NRL Memorandum
Report 6895

9. SPONSORING/MONITORING AGENCY NAME(S) AND ADDRESS(ES)

Office of Naval Research
Arlington, VA 22217-5000

10. SPONSORING/MONITORING AGENCY REPORT NUMBER

11. SUPPLEMENTARY NOTES

12a. DISTRIBUTION/AVAILABILITY STATEMENT

Approved for public release; distribution unlimited.

12b. DISTRIBUTION CODE

13. ABSTRACT *(Maximum 200 words)*

An understanding of and the ability to analytically predict the stress and strain field ahead of a crack tip is an essential portion of understanding the fracture process. In the case of dynamic loading induced fracture, fracture may be divided into three broad categories: (1) fracture caused by a single stress wave or a small number of stress wave interactions, (2) stress wave dominated fractures caused by the complex combinations of initial, refractive and reflective stress waves and (3) fractures which occur after the kinetic energy associated with stress wave interactions is negligible. The current work examines the fracture of a three point bend specimen of A517 steel which fails by stress wave dominated brittle fracture. The Mode I stress contours during the dynamic loading transient are examined in detail. Five distinct Mode I stress contour patterns caused by the continual interactions of stress waves with increasing time are observed to occur prior to fracture.

14. SUBJECT TERMS

Dynamic fracture
Fracture mechanics Finite element

15. NUMBER OF PAGES

24

16. PRICE CODE

17. SECURITY CLASSIFICATION OF REPORT	18. SECURITY CLASSIFICATION OF THIS PAGE	19. SECURITY CLASSIFICATION OF ABSTRACT	20. LIMITATION OF ABSTRACT
UNCLASSIFIED	UNCLASSIFIED	UNCLASSIFIED	UL

CONTENTS

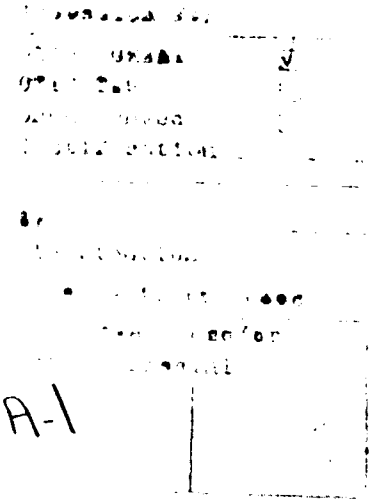

STRESS FIELD VARIATIONS DURING DYNAMIC LOADING

INTRODUCTION

Dynamic fracture is a complex phenomenon which encompasses many different types of fracture. Of interest in the current work is fracture caused by dynamic loading. Determination of the crack tip stress field is an essential portion of fracture mechanics for both static and dynamic fracture conditions. The variation in the crack tip stress field and the time to fracture are of primary concern in dynamic fracture. In the current work finite element methods are used to determine the magnitude and variation in the Mode I opening stress field surrounding a crack tip from zero load to fracture for a dynamic tear test three point bend specimen.

The stress field caused by dynamic loading conditions is the result of the interactions between individual stress waves, including combinations of dilatational, distortional and Rayleigh surface waves [1]. While the problem of the reflection of a single stress wave normal to a free surface can be considered to be relatively simple, the presence of multiple incident stress waves, curved and angled free boundaries and varying angles of impact and reflection result in extremely complicated numerical representations of stress components. If fracture occurs prior to any interactions between stress waves or when only a limited number of stress wave interactions have occurred, as in flyer plate or Hopkinson bar experiments [2], detailed analytical evaluations can be carried out for simple test geometries since relatively few stress waves are involved in the fracture process. However, if dynamic loading induced fractures occurs only after a large number of interactions between individual stress waves, the stress and strain fields at fracture result from numerous combinations of stress waves and analytical evaluations are extremely complex and cumbersome. In addition to the interaction of stress waves, the magnitude of the time to fracture must be considered in any analytical evaluation. As the time to fracture increases, the importance of individual stress waves diminishes until a time to fracture is reached where the kinetic energy becomes insignificant and it is possible to use static based solution methods to predict fracture [3].

Between these two extremes are dynamic fractures which require more than the initial stress wave or a relatively few combinations of stress waves but in which the kinetic energy is not negligible at fracture. In these cases the process of dynamic fracture can be considered to be stress wave controlled. In this intermediate

Manuscript approved July 29, 1991.

regime of dynamic fracture the changes in stress and strain at the crack tip with time are essential in the understanding and subsequent prediction of dynamic fracture. The dynamic tear three point bend test to be evaluated is a stress wave controlled fracture experiment [4].

Stress field patterns have been experimentally obtained for dynamic growing cracks under a variety of dynamic loading conditions. Among the stress patterns experimentally observed are the full field stress patterns for Homalite-100 [5], PMMA [6], low carbon type steel [7], various aluminum alloys [8] and 4340 steel [9]. A variety of specimen geometries, loadings and crack configurations have been studied. The incremental changes in contours recorded are dependent on the sampling and recording rate of the equipment used.

In the current work, the stress variation with time around the crack tip is numerically determined for the dynamic tear test using finite element techniques. Since extremely small time steps are possible, a computational evaluation of stress patterns will allow a more detailed stress pattern history to be developed than has been presented to date. The finite element model results of individual stress components are compared with analytically determined stress components during the early stages of dynamic loading to demonstrate the accuracy of the finite element model, procedures and subsequent results.

The three point bend specimen used in the dynamic tear test is shown in Figure 1. The specimen is designed so that the drop hammer hitting the unnotched side causes Mode I fracture at the crack tip. The finite element program ABAQUS is used for the finite element analysis. Plane strain 2D modeling techniques are used. The specimen is fabricated of A517 structural steel.

COMPUTATIONAL ANALYSIS

Determination of Stress Wave Domination

The focus of the current work is to examine the stress field variations due to dynamic loading in a three point bend specimen of A517 steel from initial loading to fracture initiation. The dynamic fracture regime of interest is stress wave dominated fracture.

For an initial period of time after dynamic loading, individual stress waves dominate the stress field at the crack tip. As the time from initial loading increases, the stress field formed around the crack tip stabilizes. The additional arrival of individual stress waves causes negligible variation. The time at which individual stress waves result in negligible variation in the stress field is the transition time, t_T [3]. The transition time is not an absolute value but a range which depends on specimen material and geometry. An approximation for the transition time for three-point bend specimen presented by Nakamura et al [3] is:

$$t_T = 27 \frac{H}{c_1} \tag{1}$$

where H is the specimen width and c_1 is the dilatational wave speed. This approximation has been shown to compare favorably with more rigorous definitions of the transition time [3].

The transition time defined by equation (1) for the specimen used in the current analysis is 192 x 10^{-6} seconds. The experimentally observed time to fracture is 70 x 10-6 seconds. Since the transition time is greater than the experimental fracture time, the dynamic fracture of the given specimen geometry is dominated by individual stress waves.

Experimental Load-Time History

An experimental load-time history was used as the loading function for the finite element dynamic analysis. Impact tests leading to the brittle fracture of A517 steel dynamic tear specimens have been performed and the history of the impact force measured [10]. The time span of interest is defined by the start of loading and the experimentally observed occurrence of fracture. During this time span the load can be represented as a smooth function with one local and global maximum. The load-time relationship used is shown in Figure 2.

In earlier work performed by Brock, Jolles and Schroedl [11] it was determined that the load curve could be accurately represented by a line load which is uniform across the specimen width:

$$P(s) = \frac{F_0}{c_1} s\left[1+\frac{3}{10}\left[\frac{s}{s_p}\right] +\frac{8}{15}\left[\frac{s}{s_p}\right]^2\right] \qquad (2)$$

where s=0 is the start of impact, s_p corresponds to the instant of peak impact force, and c_1 is the dilatational wave speed in the specimen. For the current geometry, material and loading history s_p = 0.35, c_1=5790 m/sec and F_0=1.4 x 10^5 MN/m-sec [4]

Finite Element Model

The finite element code ABAQUS [12] is used for the computational analysis of the dynamic tear test. Geometric and loading symmetry allow for half of the specimen to be modeled. The finite element mesh consists of 820 nodes and 760 4-noded plane strain elements and is shown in Figure 3. The elements used have linear displacement interpolation and an independent hydrostatic stress component [13]. This component is coupled to the constitutive relationship for the specimen material by LaGrange multipliers. The use of this type of hybrid element in regions of large deformations eliminates artificially stiffening of the finite element model.

The test specimen is modeled as a simply supported beam fixed in the longitudinal direction at one end. The line load of equation (1) is dynamically applied. In order to avoid localized element crushing, the line load is represented as a uniform pressure spanning two elements (4.4 mm). The three point bend specimen is 178 mm long, 41 mm deep and 16 mm thick.

It should be noted that the mesh does not include special elements that could model a crack tip, i.e., notch singularity.

ABAQUS uses an implicit integration scheme to determine dynamic response. The time steps for implicit integration schemes may become extremely large. The local truncation error for implicit integration schemes is of the order of Δt^3 [13] and may become large enough to affect the solution accuracy for larger time steps. Therefore, the time step size is limited by concerns of local solution accuracy. ABAQUS can automatically limit the time step size based on the local equilibrium residuals. By monitoring the residuals from the equilibrium equations at time $t+\Delta t/2$ the accuracy of the solution at time $t+\Delta t$ can be assessed. The time step

can be reduced if necessary and the incremental solution repeated with the smaller time step.

The program ABAQUS uses the Hilber-Hughes-Taylor single parameter operator [13] for additional user defined solution stability control. The Hilber-Hughes-Taylor allows for user variation in the amount of damping possible. Numerical damping is required with variable times steps because of the slight amount of high frequency numerical noise which is almost always introduced when the time step size changes. This noise is removed rapidly by including a small amount of damping in the the numerical integration scheme. In the current analysis a damping factor of -0.05 is used.

A maximum allowable time step is determined from the characteristic dimensions of the mesh and the material wave speed. The maximum allowed time step is:

$$\Delta t = \frac{d^*}{c_1} \tag{3}$$

where c_1 is the dilatational wave speed and d^* is the minimum dimension of the smallest element in the mesh. The time steps used are consistent with accepted dynamic finite element analysis methods [14].

Even though a brittle fracture response is expected, geometric nonlinearities are incorporated into the finite element model. Large strain solution procedures are used which will accommodate any localized large strain or rotations which may occur at the crack tip or at the impact loading site. A primary concern is the accommodation of large strains at the impact loading site. The use of large displacement solution as well as spreading the impact loading over two elements avoids localized stability problems which may result from the numerical representation of the impact load. The properties of A517 steel used are:

Young's modulus - 206.8 GPa
Shear modulus - 75.8 GPa
Poisson's ratio - 0.27
Dilatational wave speed - 5790 m/s
Rotational wave speed - 3147 m/s

Finite Element Analysis Results

The dynamic transient analysis consisted of 246 time steps of 0.33 x 10^{-6} seconds each for a total analyzed time of 81.18 x 10^{-6} seconds. Time steps which were small with respect to the total transient time were used to guarantee solution stability. Prior to any dynamic transient solution a static solution for the experimental load-time history was performed to identify and correct any errors in the model, boundary condition or loading definition.

In order to determine the accuracy of the finite element dynamic analysis results, stress component values for times prior to the arrival of reflective waves are compared with a previously determined analytical solution valid for this time period [4]. The comparison of the opening mode stresses (σx) is shown in Figure 4.

As the time into the transient increases, the difference between analytical and computational results dramatically increases. The variation starts at approximately the time of arrival of the first reflective wave. The variation in the two solutions is caused by the inclusion of reflective stress waves in one solution (the finite element solution) and the exclusion of these stress waves from the other solution (the analytical solution). This behavior has been previously predicted and observed [11,15].

In the current work, fracture and failure are considered to be synonymous. Because of the brittle nature of the A517 dynamic tear tests being modeled, the linear elastic stress intensity factor, K_I, is an appropriate fracture parameter. Fracture is defined as occurring at the experimentally observed fracture time. In order to determine if the stresses calculated by the finite element analysis are sufficient to cause fracture the opening mode critical stress intensity factor, K_{IC}, is determined. The stress intensity factor for the coordinate system used in the mesh is [16]:

$$K_I = \lim_{r \to 0} \frac{\sqrt{2\pi r}}{f(\theta)} \sigma_x \qquad (4)$$

$$f(\theta) = \cos\frac{1}{2}\left(\frac{\pi}{2} - \theta\right)\left[1 + \sin\frac{1}{2}\left(\frac{\pi}{2} - \theta\right)\sin\frac{3}{2}\left(\frac{\pi}{2} - \theta\right)\right]$$

The displacement at the crack tip was determined by extrapolation of displacement results from the finite element model near the crack tip for the load step corresponding to the fracture time. The finite element estimated K_{IC} is 144 MN/m^2.

The critical value of K_{IC} determined from the finite element *simulation is* greater than original estimates of A517 steel presented by Brock, Schroedl and Jolles [11]. However, the range defined by [11] is based on zero velocity extrapolation of stress intensity factor data obtained for growing cracks. Experiments similar to the dynamic tear test represented by the finite element analysis have been performed for 4340 steel [17]. The K_{IC} range determined for 4340 steel is 200-250 MN/m^2. The estimated K_{IC} for A517 is less than these values but greater than zero velocity K_{IC} for A517.

The value of K_{IC} determined from the finite element analysis indicates that stresses and strains in the finite element analysis have reached a level required for fracture.

Support Constraints

In the initial stages of the load-time history the three point bend specimen is observed to lift off of its supports. This is consistent with previous observations [18]. The boundary conditions used in the analyses do not allow the specimen to lift off from it's supports. The resulting reaction forces have a negligible influence on the crack tip stress fields.

Spatial Variations in Stress Contours

The stress contours surrounding a crack tip are as important as the magnitude of the stresses in the understanding of dynamic fracture. The variations in stress magnitudes and patterns with time is partially due to the interaction of reflective stress waves. The importance of reflective stress waves in the development of critical fracture stresses and strains has been observed both experimentally [5] and analytically [4]. Reflective stress waves are included in the finite element full field stress solution.

The variations in the stress contours for a small region around the crack tip are described in detail. The region near the crack tip

which is examined in detail is 13 mm by 13 mm. The notch tip is centered in the y-direction. The x-direction extent is measured from the specimen center plane.

It is possible to divide the changes in the opening mode stress contours at the crack tip into five distinct stages based on stress field magnitudes and geometric characteristics. Each stage is representative of a range in time during the transient. There is a gradual transition from a state of no stress to a stress concentration pattern which is similar to what would be observed at a crack tip subjected to static loading. The spatial variation of the opening mode stress stabilizes to the static stress concentration pattern relatively early in the transient. After the pattern has become stabilized the opening mode stress is observed to monotonically increase in magnitude.

During the initial stage the impact wave has not yet had time to reach the notch tip region.

The beginning of the second stage is defined by the arrival of the initial impact wave. The initial impact wave arrives at a point near the crack tip ($r=1.32$ mm, $\theta=0$) 4.9×10^{-6} seconds. This stage is characterized by a uniform stress pattern near the crack tip, as seen in Figure 5, for a transient time of 5.1×10^{-6} seconds. The stress pattern shows smooth variation in the y-direction ahead of crack tip. The variation between stage one and stage two is minor in terms of contour patterns but critical in terms of the stress magnitude and location of the initial stress wave.

The beginning of the third stage is defined by the arrival of the first reflective wave. The time to arrival at a point near the crack tip ($r=1.32$ mm, $\theta=0$) is 9.4×10^{-6} seconds. The third stage is characterized by apparently chaotic variations in the stress patterns due to the interaction of refractive and reflective stress waves. The changing nature of the opening mode stress contours characteristic of this time period is typified by the contours shown in Figure 6a and 6b for 9.9×10^{-6} and 11.4×10^{-6} seconds, respectively. The lack of stress field stabilization and lack of stress field self-similarity are important features of this transitional stage. The effect of the arrival of the first and subsequent reflective waves on the magnitude of the opening mode

stress can be seen in Figure 4; the variation in the two solutions shown is due solely to the effects of reflective waves.

The fourth stage begins at approximately 16.0 x 10^{-6} seconds when the crack tip is first observed to act as a stress concentrator and the opening mode stress pattern associated with a crack tip is first observed. The stress concentrator effect of the crack tip is fully developed by 25.0 x 10^{-6} seconds. At this time during the transient there is an order of magnitude difference between dynamic and static analysis opening mode stresses as can be seen in Figure 7. There are no changes in the stress pattern around the crack tip from the beginning of the fourth stage until fracture occurs.

The last stage of opening mode stress variation occurs just prior to fracture and is marked by a change in magnitude rather than a change in pattern. At approximately 66.0 x 10^{-6} seconds the opening mode stresses are similar to the static analysis opening mode stresses in both appearance and magnitude (Figure 8). Fracture is experimentally observed to occur at approximately 70.0 x 10^{-6} seconds.

SUMMARY

Because the time to fracture is less than the transition time, the fracture process for the three point bend specimen of A517 steel is dominated by the stress wave phenomenon. The critical stress level is achieved by the complicated interaction of the impact, refractive and reflective stress wave. The time to fracture is dependent on the stress wave response. The arrival times of stress waves are dependent on both material wave speed and distance to travel. The fracture is stress wave dominated. The time to fracture is dependent on material characteristics, such as wavespeed, and specimen geometry. The stress wave phenomenon results in five distinct stages of Mode I stress pattern development prior to fracture. The formation of classical Mode I stress patterns occurs well before fracture initiation time.

REFERENCES

1. Kolsky, H., "Recent Work on Relations between Stress Pulses and Fracture," Dynamic Crack Propagation, Sih, G. C., ed., Noordhoff, Leyden, 1973.

2. Goldsmith, W. G., Impact, Edward Arnold (Publishers) Ltd., London, England, 1960.

3 Nakamura, T., Shih, C. F, and Freund, L. B., "Analysis of a Dynamically Loaded Three-Point-Bend Ductile Fracture Specimen," Engineering Fracture Mechanics, Vol. 25, No. 3, 1986.

4. DeGiorgi, V. G. and Brock, L. M., "The Effect of First Reflections in the Dynamic Tear Test," J. of Eng. Mechanics, Vol. 116, No. 6, 1990.

5. Kobayashi, A. S. and W. G. Wade, "Crack Propagation and Arrest in Impacted Plates," Dynamic Crack Propagation, Sih, G. C., ed., Noordhoff, Leyden, 1973.

6. Radon, J. C. and Fitzpatrick, "Deformation of PMMA at High Rates of Strain," Dynamic Crack Propagation, Sih, G. C., ed., Noordhoff, Leyden, 1973.

7. van Elst, H. C., "The Relationship Between Increase in Crack Arrest Temperature and Decrease of Stress Wave Attenuation by Material Embrittlement," Dynamic Crack Propagation, Sih, G. C., ed., Noordhoff, Leyden, 1973.

8. Dadkhah, M. S. and A. S. Kobayashi, "An Experimental Analysis of a Moving Ductile Crack", Developments in Mechanics, Vol. 15, Michigan Technological University, Michigan, 1989.

9. Zehnder, A. T. and Rosakis, A. J., "Dynamic Measurement of the J Integral in Ductile Metals Using Optical Method of Caustics," Proceedings Twelfth Canadian Congress of Applied Mechanics, Ottawa, Ontario, 1989.

10. Nash, G. E. and Lange, E. A., "Mechanical Aspects of the Dynamic Tear Test," ASME Journal of Basic Engineering, Vol. 91, 1969.

11. Brock, L. M., Jolles, M., and Schroedl, M., "Dynamic Impact over a Subsurface Crack: Applications to the Dynamic Tear Test," ASME Journal of Applied Mechanics, Vol. 52, 1985.

12. Hibbitt, H. D., Karlsson, B. I., and Sorensen, E. P., ABAQUS User's Manual, Hibbitt, Karlsson and Sorensen, Inc., Providence, RI, 1984.

13. Hibbitt, H. D., Karlsson, B. I., and Sorensen, E. P., ABAQUS Theory Manual, Hibbitt, Karlsson and Sorensen, Inc., Providence, RI, 1984.

14. Zukas, Jonas,A., "Numerical Simulation of Impact Phenomena," Impact Dynamics, John Wiley and Sons, New York, NY, 367-417, 1982.

15. Brock, L. M., and Rossmanith, H. P., "Analysis of the Reflection of Point Force-Induced Crack Surface Waves by a Crack Edge," ASME Journal of Applied Mechanics, Vol. 52, 1985.

16. Broek, D., Elementary Engineering Fracture Mechanics, Matinus Nijhoff, Boston, MA, 1982.

17. Zehnder, A. T. and Rosakis, A. J., "Dynamic Fracture Initiation and Propagation in 4340 Steel Under Impact Loading," SM Report 86-6, Graduate Aeronautical Laboratories, California Institute of Technology, 1986.

18. Crouch, B. A. and Williams, J. G., "Modelling of Dynamic Crack Propagation Behavior in the Three Point Bend Impact Specimen," J. Mech. Physics and Solids, Vol. 36, No. 1, 1988.

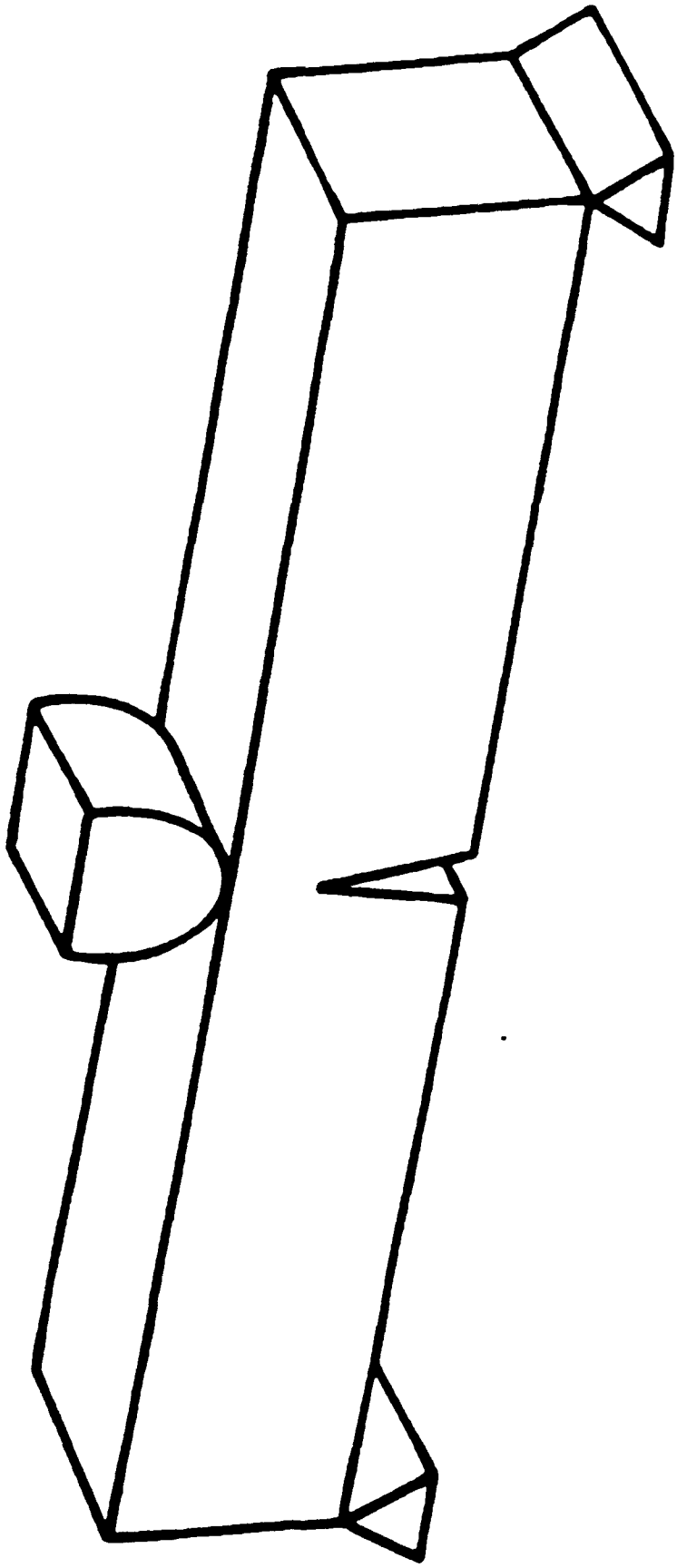

Fig. 1 — Three Point Bend Specimen Geometry

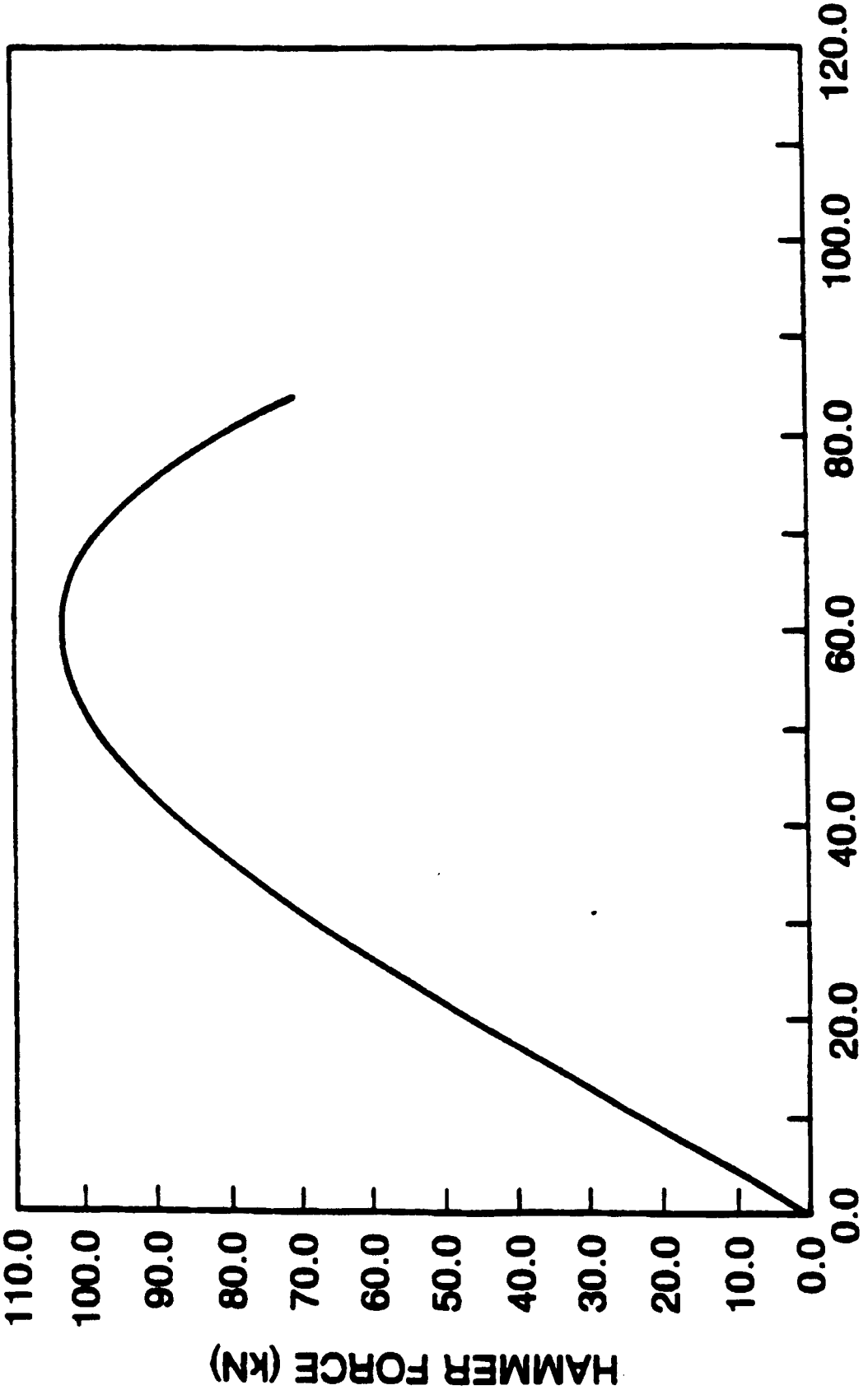

Fig. 2 — Experimental Dynamic Tear Test Load-Time Histogram

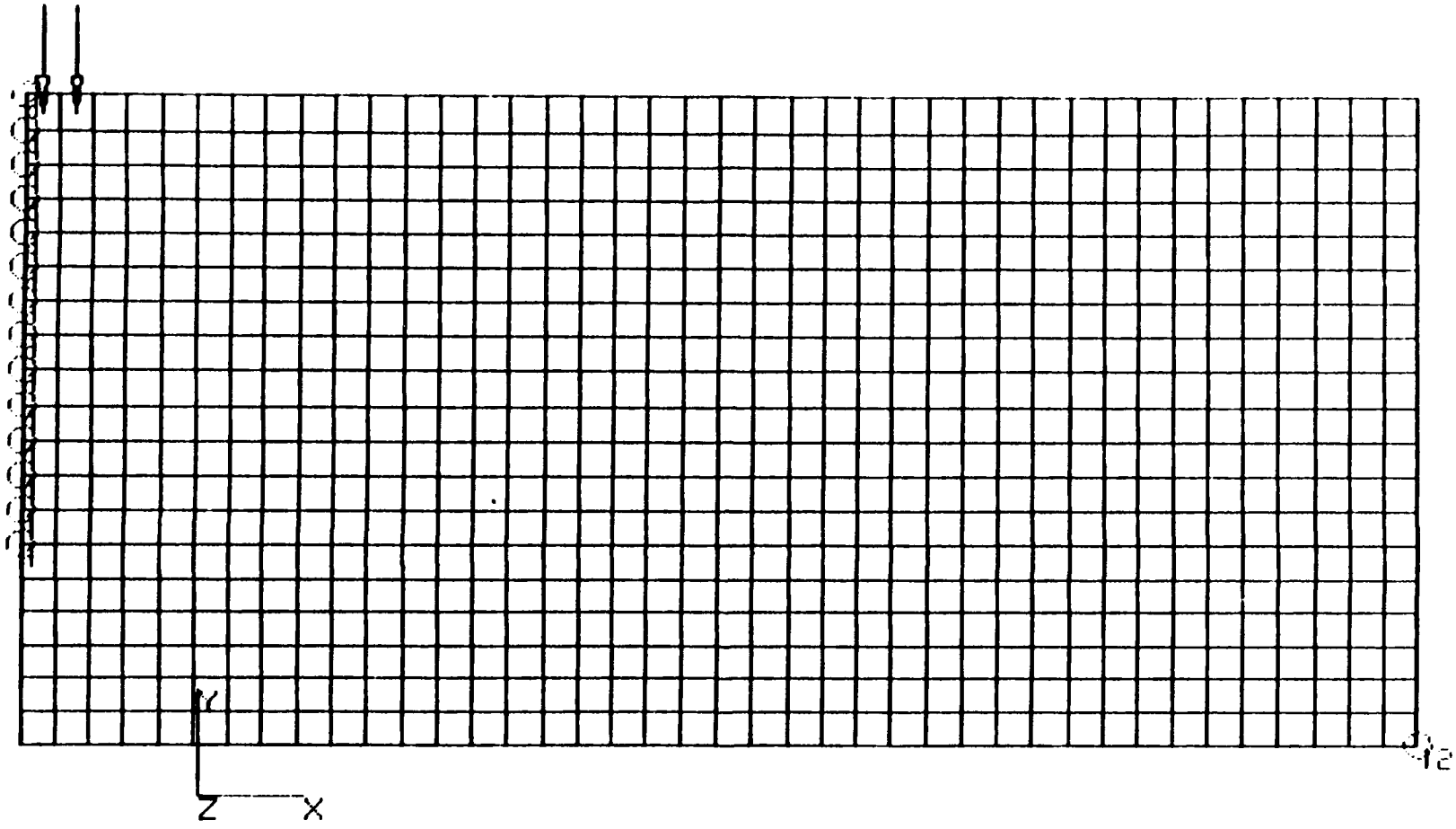

Fig. 3 — Three Point Bend Specimen Finite Element Mesh

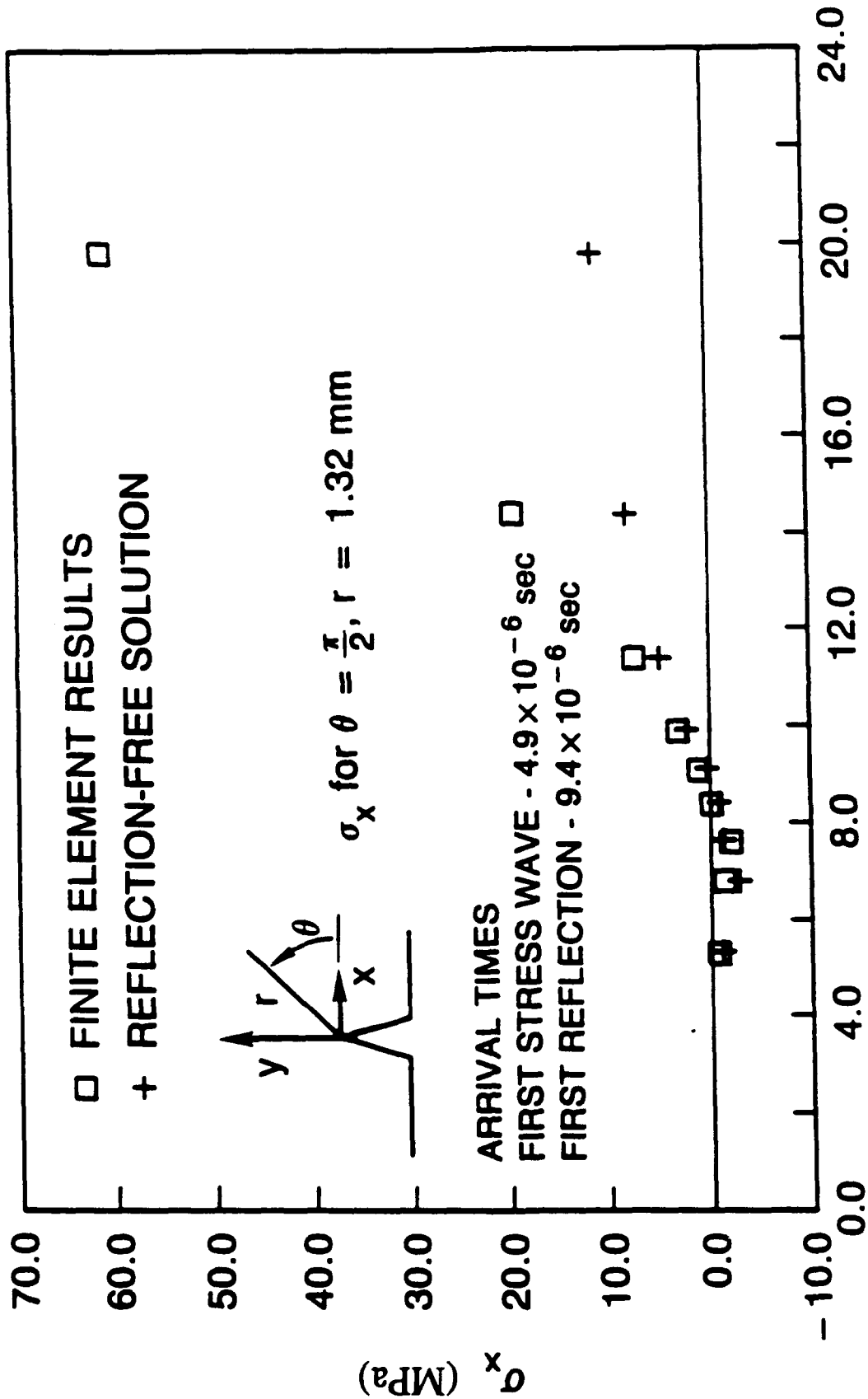

Fig. 4 — Comparison of Analytical and Computational Opening Mode Stress Component

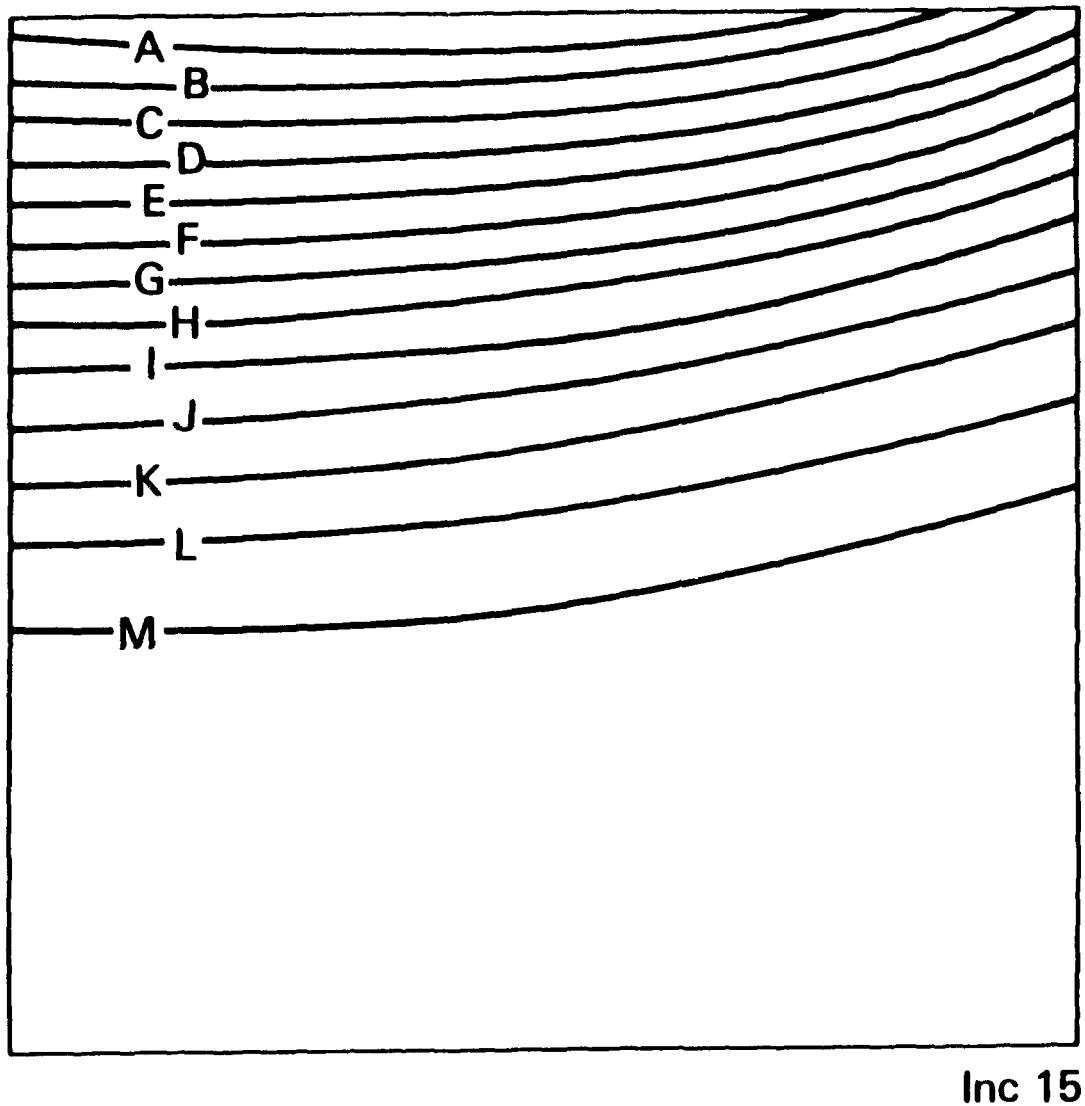

Mode I Stress (MPa)

A	-1.5
B	-1.4
C	-1.3
D	-1.2
E	-1.1
F	-1.0
G	-0.8
H	-0.7
I	-0.6
J	-0.5
K	-0.4
L	-0.3
M	-0.2

Fig. 5 — Opening Mode Stress Levels at 5.1×10^{-6} seconds

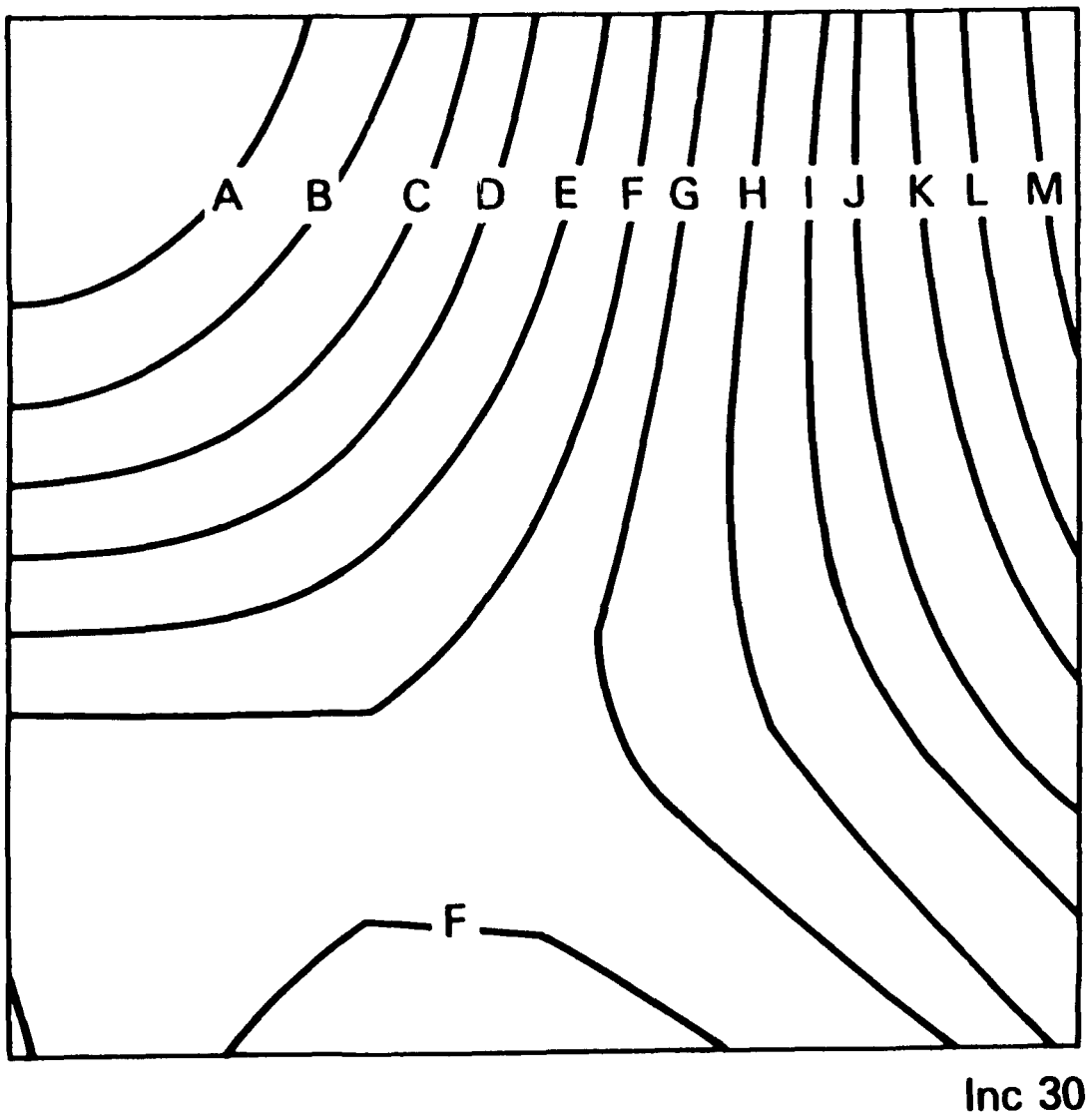

Mode I Stress (MPa)

A	-3.9
B	-3.3
C	-2.8
D	-2.1
E	-1.6
F	-1.0
G	-0.4
H	0.2
I	0.8
J	1.4
K	1.9
L	2.6
M	3.1

Fig. 6a — Opening Mode Stress Levels at 9.9×10^{-6} seconds

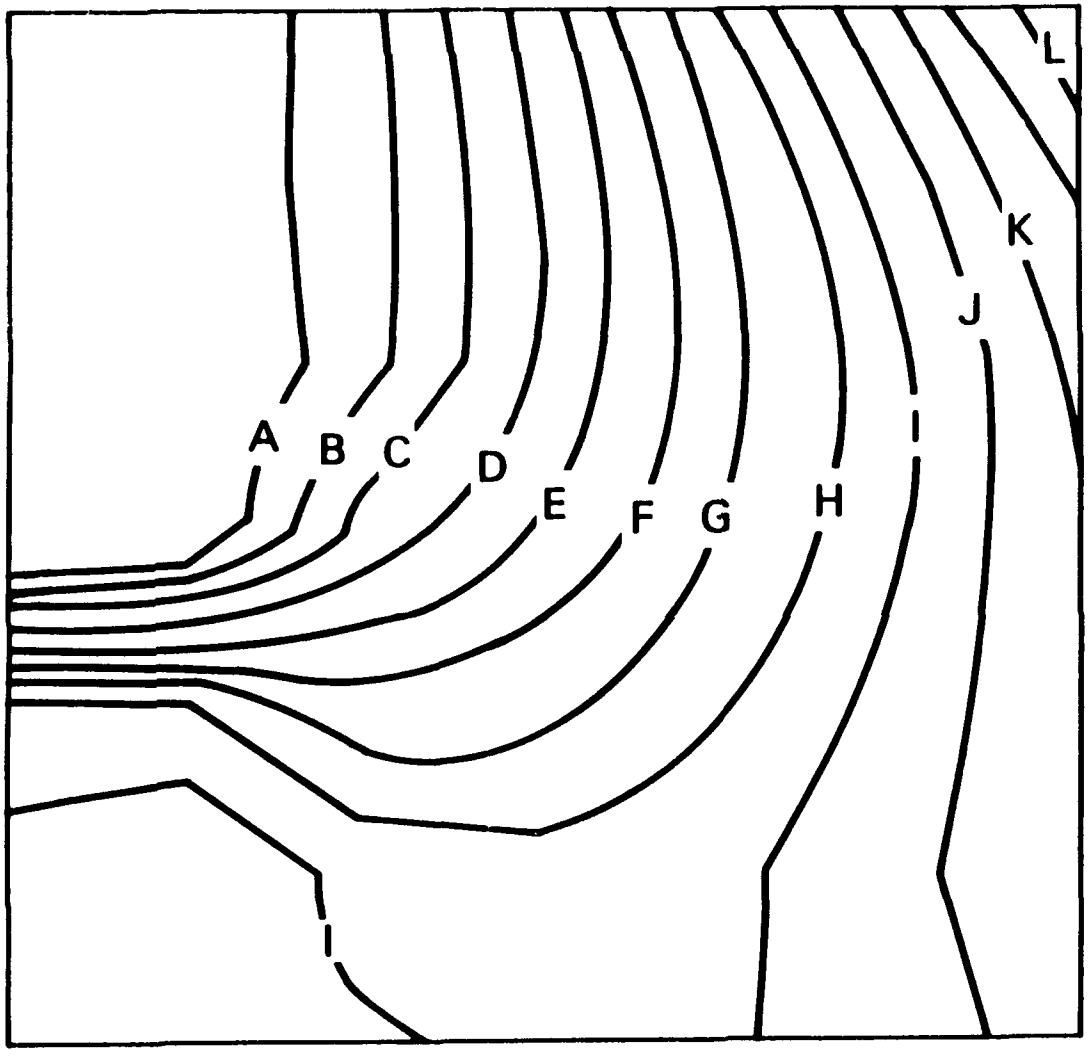

Mode I Stress (MPa)

A	6.1
B	5.5
C	4.8
D	4.2
E	3.5
F	2.9
G	2.2
H	1.6
I	0.9
J	0.3
K	-0.4
L	-1.0
M	-1.7

Fig. 6b — Opening Mode Stress Levels at 11.4×10^{-6} seconds

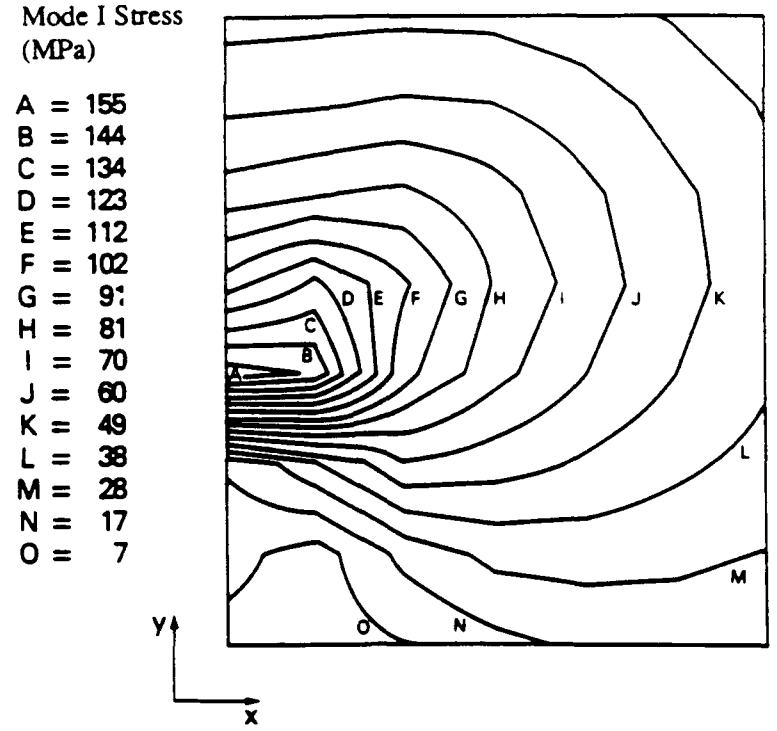

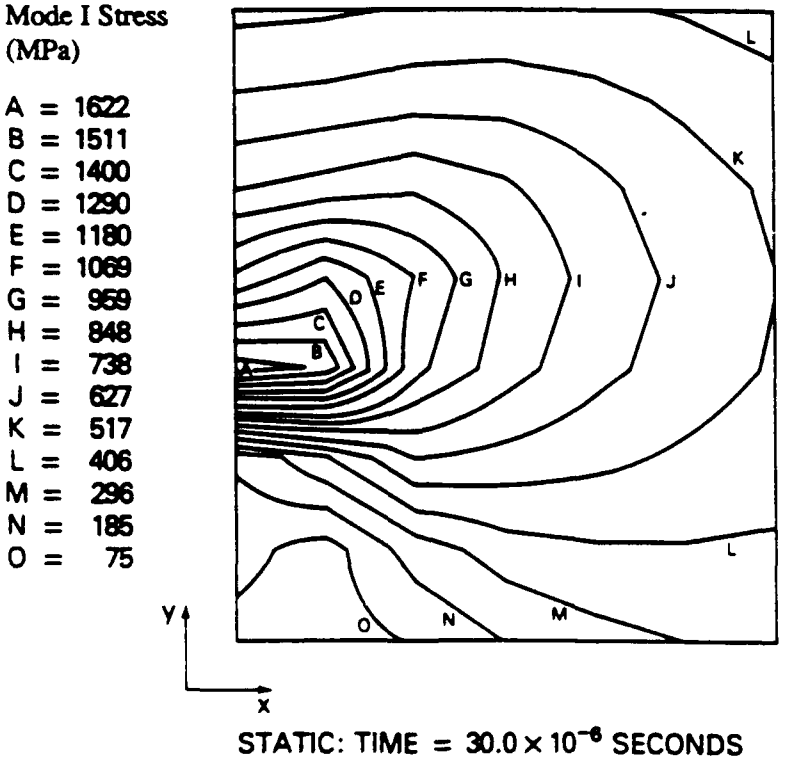

Fig. 7 — Comparison of Static and Dynamic Loading Opening Mode Stress Contours

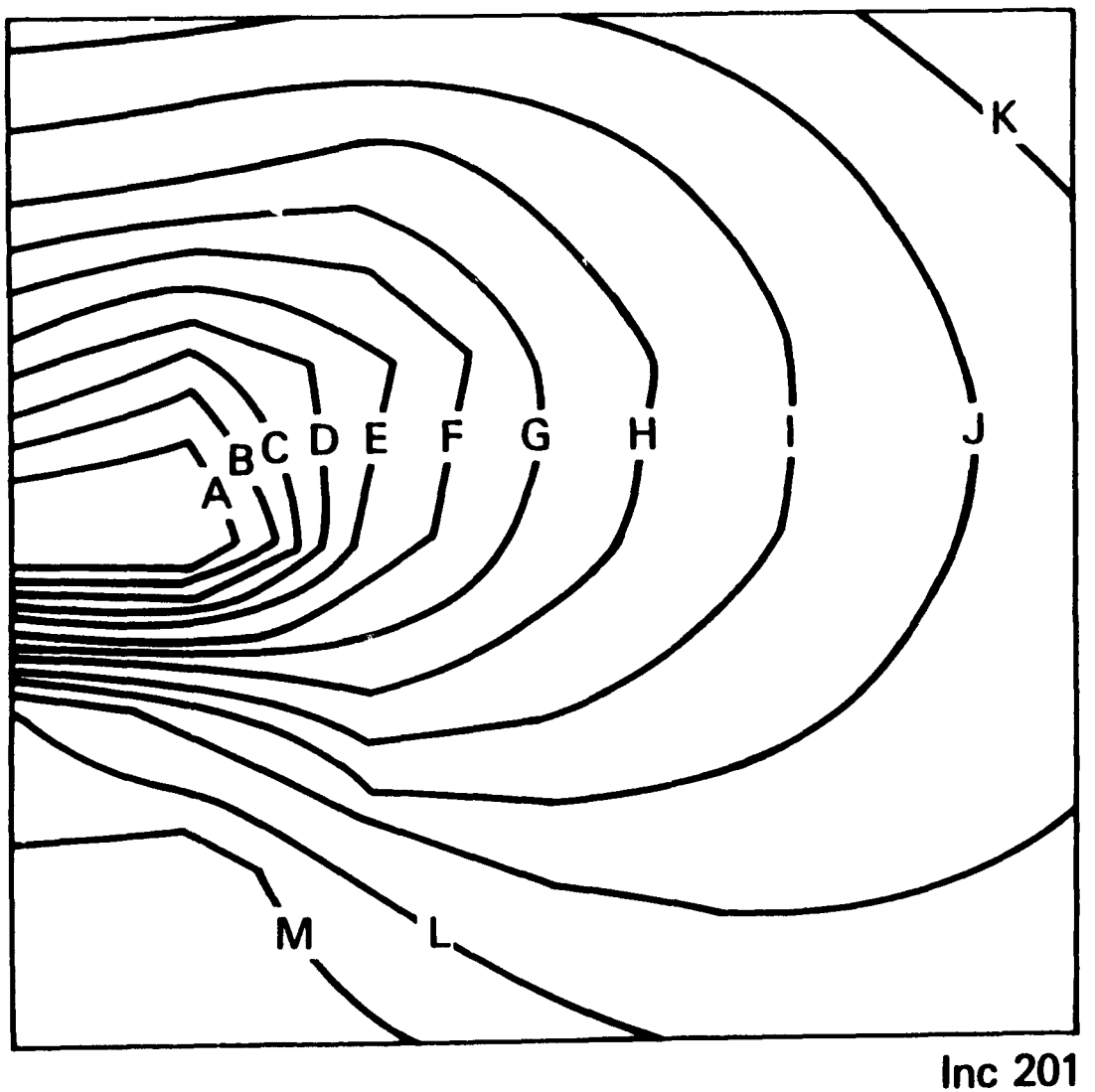

Mode I Stress (MPa)

A	583.7
B	539.4
C	495.2
D	451.0
E	406.8
F	362.6
G	318.3
H	274.1
I	229.9
J	185.7
K	141.5
L	97.2
M	53.0

Fig. 8 — Opening Mode Stress Levels at 66.0 × 10^{-6} seconds